Composition dependent selectivity in the coadsorption of H_2O and CO on pure and binary silver–gold clusters

Irene Fleischer [a], Denisia M. Popolan [a], Marjan Krstić [b], Vlasta Bonačić-Koutecký [b,c,*], Thorsten M. Bernhardt [a,*]

[a] Institute of Surface Chemistry and Catalysis, University of Ulm, Albert-Einstein-Allee 47, 89069 Ulm, Germany
[b] Interdisciplinary Center for Advanced Sciences and Technology (ICAST), University of Split, Meštrovićevo, Šetalište bb., 2100 Split, Croatia
[c] Chemistry Department, Humboldt University of Berlin, Brook-Taylor-Strasse 2, 12489 Berlin, Germany

ARTICLE INFO

ABSTRACT

Small cationic gold clusters exhibit a strong affinity toward carbon monoxide. This prevents the coadsorption of water which would be the first step of a catalytic water gas shift chemistry on these clusters. In a gas phase ion trap experiment with mass selected $Ag_nAu_m^+$ it was however possible to demonstrate that the replacement of gold by silver atoms in triatomic cluster ions liberates sites for H_2O adsorption. The resulting observed coadsorption effect occurs at a cross-over in the molecular binding energies of carbon monoxide and water to these clusters determined by reaction kinetics measurements and first principles calculations.

1. Introduction

There is currently a strong interest in the properties of intermetallic compounds with finite nanoscale dimensions which are often conveniently termed 'nanoalloys' [1]. With respect to the reactive properties of such small alloy particles in heterogeneous catalysis recent results show surprising activities and in particular product selectivities that clearly deviate from those of the pure constituent metal compounds [2–4].

Gas phase experiments with mass-selected clusters can contribute to gain molecular level insight into the mechanistic origin of such new chemical properties of nanoalloy metal particles [5]. In addition to the exactly defined size also the composition can be varied atom by atom in such small clusters and thus detailed trends in the chemical reactivity can be revealed [6–10].

In this contribution we explore the possibility to tune the reactive properties of triatomic gold cluster cations by 'alloying' with silver. Small positively charged gold clusters are known to strongly bind carbon monoxide [9–13] which prevents the coadsorption of many other ligands. Here, we are interested in the interaction of CO with water in a water gas shift reaction scheme:

$$H_2O + CO \rightleftarrows CO_2 + H_2 \tag{1}$$

This reaction is technically important for the production of hydrogen and the removal of noxious CO impurities in, e.g., fuel cell feed gases. In the water gas shift reaction the coadsorption of CO and H_2O on the catalyst represents the necessary first reaction step, followed by activation of the ligands and the subsequent actual chemical transformation. Previous studies already indicated that the replacement of gold by silver atoms leads to a weaker bonding of CO to the clusters [10,11,13].

In the following we present the first investigation (experimental and theoretical) of the coadsorption of water with carbon monoxide as a function of the composition of binary silver–gold cluster cations. The results reveal that the adsorption of both molecules is indeed possible on Ag_2Au^+ and that this effect can be related to a cross-over in the binding energies of these molecules to the clusters of different composition.

2. Methods

The reaction between mass-selected cluster ions and neutral reactant gases without the influence of a surface were investigated in a gas phase low energy ion beam setup that includes a radio frequency (rf) octopole ion trap inserted into a system of quadrupoles to guide the ions and a quadrupole mass spectrometer to detect the products. This experimental layout has been described in detail elsewhere [14–16] and will only be described briefly here. In addition to the data acquisition routine a concise summary of the data

---

* Corresponding authors. Addresses: Chemistry Department, Humboldt University of Berlin, Brook-Taylor-Str. 2, 12489 Berlin, Germany. Fax: +49 (0)30 2093 5573, and Interdisciplinary Center for Advanced Sciences and Technology (ICAST), University of Split, Meštrovićevo, Šetalište bb., 2100 Split, Croatia (V. Bonačić-Koutecký), Institute of Surface Chemistry and Catalysis, University of Ulm, Albert-Einstein-Allee 47, 89069 Ulm, Germany. Fax: +49 (0) 731 50 25452 (T. M. Bernhardt).

E-mail addresses: vbk@chemie.hu-berlin.de (V. Bonačić-Koutecký), thorsten.bernhardt@uni-ulm.de (T.M. Bernhardt).

evaluation methods will be given in the following. Finally, the computational methods will be described.

2.1. Data acquisition

The sputtering of metal-alloy targets (70 wt.% Ag, 30 wt.% Au) with a cold reflex discharge ion source (CORDIS [17]) was employed to generate the metal cluster cations. The cluster ions were thermalized by collisions with helium gas, mass-selected by a first quadrupole filter and subsequently guided to the octopole ion trap which was filled with about 1 Pa helium buffer gas and small partial pressures of reactant gas. The total pressure inside the ion trap was measured by a Baratron gauge (MKS, type 627B). The temperature of the trap could be varied between 20 and 300 K by resistive heating against an attached helium cryostat. Thermal equilibration of the clusters was achieved under these experimental conditions within a few milliseconds [15]. After a defined reaction time, i.e. storage time inside the trap, the products were extracted and analyzed with a further quadrupole mass filter. By recording all the product ion concentrations as a function of the reaction time, the kinetics of the reaction could be measured.

2.2. Data evaluation

To determine the binding energies of the carbonyl ligands to the metal clusters the thermodynamic equilibrium evaluation method was used (see Ref. [10] and references therein). This method is based on temperature dependent measurements of the reactions of interest under thermodynamic equilibrium conditions.

Yet, the reaction experiments with water as reactant gas could be performed reliably only at room temperature because of condensation effects that occurred, if the trap was held at a different temperature than the gas inlet. Therefore, room temperature kinetics measurements were performed in the case of the reaction between the metal clusters and water and statistical reaction rate analysis employing the Rice-Ramsperger-Kassel-Marcus (RRKM) method was applied to determine the water binding energies [18,19]. Details of the statistical kinetics evaluation procedure and of the corresponding error analysis have been described elsewhere [10,16] and thus only a summary of this method to obtain ligand binding energies will be given in the following.

For the analysis of the metal cluster reactions with H_2O simple association reactions according to Eq. (2) were assumed to proceed in the ion trap.

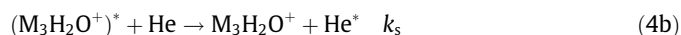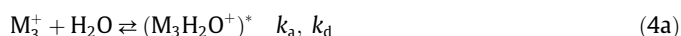$$M_3^+ + H_2O \rightarrow M_3H_2O^+ \tag{2}$$

During the reaction the concentration of the reactive gas in the octopole ion trap was orders of magnitude larger than the metal cluster ion concentration and a steady flow of the reactants was ensured. Hence, the concentration of the reactive gas was considered to remain constant in the data evaluation procedure. Consequently, the association reaction (2) was assumed to follow pseudo-first-order kinetics with the rate constant k. The reaction kinetics was evaluated by fitting the integrated rate equations of the mechanism Eq. (2) to the normalized experimental kinetic data [19]. The pseudo-first-order rate constant k contains the termolecular rate constant $k^{(3)}$ as well as the concentrations of the helium buffer gas and the reactive gas (Eq. (3)).

$$k = k^{(3)}[He][H_2O] \tag{3}$$

Thus, the termolecular rate constant can be obtained from the experimentally determined pseudo-first-order rate constant k and the partial pressures of Helium buffer gas and water (after correction for thermal transpiration [16,20–23]). As the total pressure inside the trap was about 1 Pa the reactions were performed in the

kinetic low-pressure regime. Therefore, an energy transfer mechanism has to be considered for the overall association reaction Eq. (2) to occur [19]:

$$M_3^+ + H_2O \rightleftharpoons (M_3H_2O^+)^* \quad k_a, k_d \tag{4a}$$

$$(M_3H_2O^+)^* + He \rightarrow M_3H_2O^+ + He^* \quad k_s \tag{4b}$$

The energy transfer mechanism consists of three elementary steps including the formation of an energized complex $(M_3H_2O^+)^*$ in the first association step with the rate constant k_a. The reverse dissociation reaction with the rate constant k_d describes the potential unimolecular decomposition back to the reactants. In competition with this dissociation step, the stabilization through an energy-transfer collision with a Helium atom is possible. k_s is the rate constant for the stabilization reaction.

If the steady-state approximation is considered [19], the overall third-order rate constant is given by

$$k^{(3)} = k_a k_s/(k_d + k_s[He]) \tag{5}$$

Under the given low pressure conditions the decomposition rate constant can be considered to be much larger than the stabilization rate constant ($k_d \gg k_s[He]$) resulting in a new expression for the third-order rate constant

$$k^{(3)} = k_a k_s/k_d \tag{6}$$

The association rate constant k_a and the stabilization rate constant k_s can be approximated by ion–molecule collision rate constants as specified by Langevin theory [16,19,24]. Both reactions are ion–dipole or ion-induced dipole interactions, respectively, without energy barriers.

In contrast, the unimolecular decomposition reaction with the rate constant k_d exhibits an activation energy barrier, which is associated with the molecular binding energy of the ligand to the metal clusters. k_d can be obtained from statistical reaction rate theory in the framework of the RRKM method [18,25] and thus be used to determine the H_2O binding energies E_b. For this purpose the software package 'MassKinetics' was employed to simulate the decomposition rate constant k_d on the basis of a given binding energy [26]. The vibrational frequencies of the metal clusters required in the RRKM calculations have been taken from the current theoretical results.
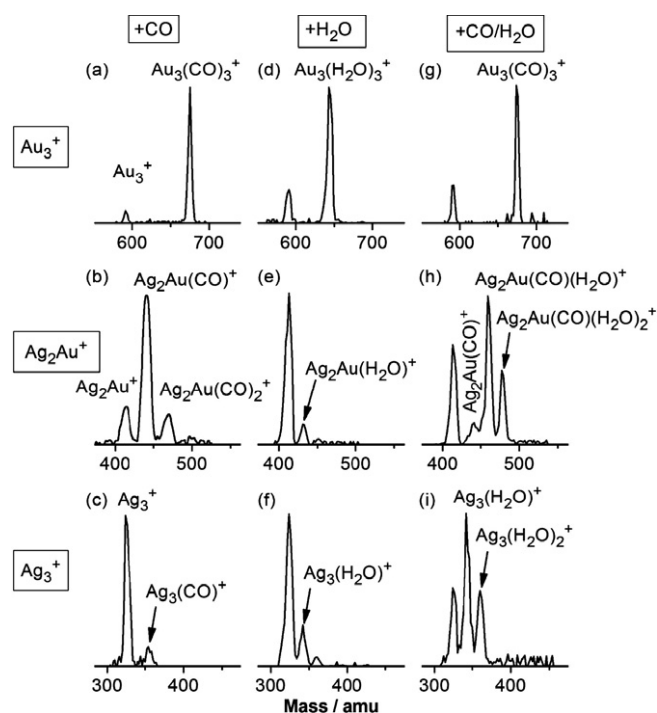
In the calculations a 'tight' and a 'loose' transition state (TS) model was assumed [16]. A 'tight' TS model describes bond rearrangement processes and results in a lower limit of E_b [16,28]. In contrast, a 'loose' TS model is usually associated with simple dissociation reactions and thus represents a more realistic model for the cluster-molecule systems investigated here. For a detailed description of the RRKM evaluation procedure please see Ref. [16].

2.3. Computational methods

The structural properties of all binary silver–gold trimer cluster complexes $Ag_nAu_m(H_2O)^+$ ($n + m = 3$) were determined using density functional theory (DFT) with the hybrid B3LYP functional [29–32]. For gold and silver atoms a triple-zeta-valence-plus-polarization (TZVP) atomic basis set combined with a 19-electron relativistic effective core potential (19e-RECP) were employed [33,34]. For the hydrogen and oxygen atoms we used the TZVP atomic basis sets [35]. All structures presented were fully optimized using gradient minimization techniques.
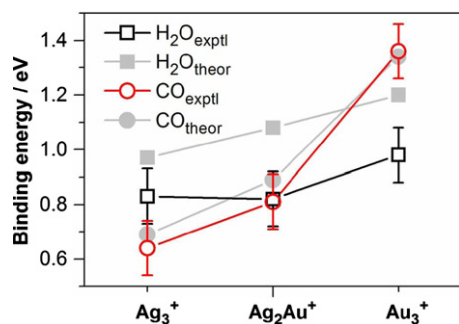
3. Results

The reactions between CO and the free gold, silver and binary silver–gold trimer clusters have been studied in our laboratories
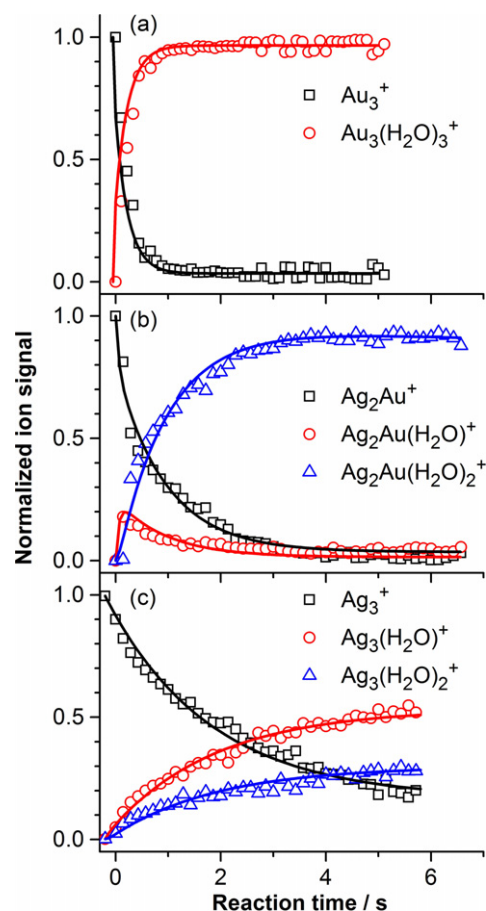
Figure 1. Product ion mass distributions measured after the reaction of Au_3^+ (a, d, g), Ag_2Au^+ (b, e, h), and Ag_3^+ (c, f, i) with CO (a–c) and H_2O (d–f) at 300 K ($p(He) = 1$ Pa; $p(CO) = 0.02$ Pa, except in (b) $p(CO) = 0.22$ Pa; $p(H_2O) = 0.003$ Pa). The spectra in the right column display product ion mass distributions obtained when both reactive molecules CO and H_2O were present in the ion trap ($p(CO) = 0.04$ Pa, $p(H_2O) = 0.004$, 300 K) for Au_3^+ (g), Ag_2Au^+ (h) and Ag_3^+ (i). All the spectra were obtained after a reaction time of 500 ms.

previously [10]. Depending on the reaction temperature all investigated trimer clusters adsorb CO in sequential equilibrium reaction steps. Figure 1a–c displays the corresponding product mass spectra obtained at room temperature and a reaction time of 500 ms. The complete kinetics and temperature dependent analysis can be found in Reference [10]. Under these conditions the pure gold cluster Au_3^+ rapidly reacts with three CO, each attached to one gold atom of the cluster, leading to the final product $Au_3(CO)_3^+$ [10]. Under similar experimental conditions, the pure silver and the binary silver–gold cluster Ag_2Au^+ react with only one CO each. If the CO pressure is increased, further CO adsorption is observed. This is shown for the case of Ag_2Au^+ in Figure 1b. The enhanced reactivity of Au_3^+ toward CO is also reflected in the composition dependent binding energy (displayed in Figure 2), which is considerably higher for Au_3^+ than for the other trimers.

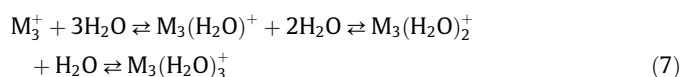**Figure 2.** Experimental and theoretical composition dependent binding energies of a first H_2O (squares, experimental values based on the 'loose' TS model) and CO (circles) molecule, respectively, to the clusters Ag_3^+, Ag_2Au^+ and Au_3^+. Binding energies of CO to the clusters have been taken from Ref. [10]. The lines connecting the data points have been drawn to guide the eye.

Figure 3. Kinetics of the reactions of Ag_3^+(a), Ag_2Au^+(b), and Au_3^+(c) with H_2O at 300 K. The open symbols represent the experimental data, normalized to the initial metal cluster concentration and to the total ion concentration in the trap. The solid lines have been obtained by fitting the integrated rate equations of the proposed reaction mechanism (Eq. (7)) to the experimental data. The experimental pressure conditions are included in Table 1.

The interaction of H_2O with Au_3^+ has been investigated previously [36]. However, no quantitative binding energies have been determined so far. Also no reaction studies of Ag_3^+ or of Ag_2Au^+ with water have been reported in the literature. Figure 1d–f displays the product mass spectra after reaction of H_2O with these trimer clusters at room temperature. The corresponding kinetic traces are depicted in Figure 3. All clusters have the capability to form adsorption products with H_2O. The pure silver cluster reacts with up to two ligands as does Ag_2Au^+. Au_3^+ is again the most reactive cluster and leads to the complex $Au_3(H_2O)_3^+$ as final product.

Experimental binding energies of the first H_2O molecule to these clusters have been determined via statistical analysis of the kinetic data in Figure 3 as described in the Methods Section. The solid lines in Figure 3 represent the best fit of the integrated rate equations to the experimental data according to the following sequential H_2O association reaction mechanism:

$$M_3^+ + 3H_2O \rightleftarrows M_3(H_2O)^+ + 2H_2O \rightleftarrows M_3(H_2O)_2^+$$
$$+ H_2O \rightleftarrows M_3(H_2O)_3^+ \qquad (7)$$

The thus obtained rate constants k for the adsorption of the first water molecule are listed in Table 1 and the resulting binding energies can be found in Table 2 for the different transition state models as detailed in Section 2.2 together with the theoretically obtained values.

From the graphical comparison of the CO and the H_2O binding energies (experimental values are displayed only for the more

Table 1

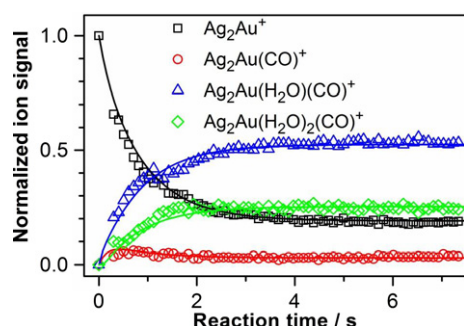Measured pseudo first order (k) and termolecular ($k^{(3)}$) rate constants for the investigated reactions of the trimer cluster cations M_3^+ with water, as well as deduced unimolecular decomposition rate constants (k_d) of the energized complexes $(M_3H_2O^+)^*$ at 300 K. Also included are the experimental pressure conditions (not yet corrected for thermal transpiration [16]) and the Langevin rate constants k_a and k_s.

M_n^+	$p(He)$ (Pa)	$p(H_2O)$ (Pa)	k (s^{-1})	$k^{(3)}$ (10^{-28} cm^{6}s^{-1})	k_a (10^{-10} cm^{3}s^{-1})	k_s (10^{-10} cm^{3}s^{-1})	k_d (10^9 s^{-1})
Ag$_3^+$	1.000	0.004	0.41 ± 0.08	19 ± 6	23.27	5.328	67 ± 22
Ag$_2$Au$^+$	1.000	0.004	1.17 ± 0.23	53 ± 17	23.13	5.322	23 ± 8
Au$_3^+$	1.011	0.005	4.0 ± 0.8	178 ± 6	22.98	5.315	0.07 ± 0.02

Table 2

Binding energies E_b of H_2O to all investigated cluster ions M_3^+ as deduced by employing RRKM theory for 'tight' and 'loose' TSs as well as DFT theory.

M_3^+	E_b (eV) exptl. 'tight' TS	E_b (eV) exptl. 'loose' TS	E_b (eV) theoretical
Ag$_3^+$	0.49 ± 0.1	0.83 ± 0.1	0.97
Ag$_2$Au$^+$	0.47 ± 0.1	0.82 ± 0.1	1.08
Au$_3^+$	0.58 ± 0.1	0.98 ± 0.1	1.20

Figure 4. Kinetics of the reaction of Ag$_2$Au$^+$ with CO and H_2O at 300 K. The open symbols represent the normalized ion signals, while the solid lines are obtained by fitting the integrated rate equations of the proposed reaction mechanism (Eq. (8)) to the experimental data.

realistic 'loose' transition state model) in Figure 2 it is apparent that a cross over occurs in the affinity of the small clusters toward these molecules as a function of the composition. Whereas CO binds more strongly to Au$_3^+$ than H_2O the reverse relative bonding behavior is observed for Ag$_3^+$. The theoretical data confirm this result as can be seen form Figure 2. The agreement between the theoretical CO binding energies and the experimental data is very favorable. Also the trend in the calculated H_2O binding energies is quite similar to the experiment. Yet, the quantitative theoretical H_2O binding energies are systematically 0.18–0.22 eV higher than the experimental values.

The major goal of this Letter was to investigate the potential coadsorption of CO and H_2O on the chosen noble metal trimers which is the mandatory first step with respect to their prospective activation and subsequent reaction in a water gas shift type chemistry. Figure 1g–i thus shows product mass spectra of the investigated clusters in the case when both reactants H_2O and CO are present in the ion trap.

No difference is detected in the presence of water compared to the result when CO is the sole reactant for Au$_3^+$. The complex Au$_3$(CO)$_3^+$ is observed as the major product. However, most surprisingly, the replacement of two gold atoms by silver in Ag$_2$Au$^+$ apparently liberates sites for the adsorption of H_2O and the coadsorption complexes Ag$_2$Au(H$_2$O)CO$^+$ as well as Ag$_2$Au(H$_2$O)$_2$CO$^+$ are detected. The corresponding kinetic data shown in Figure 4 will be discussed below. Finally, Ag$_3^+$ prefers the exclusive adsorption of two water molecules at room temperature (see Figure 1i; obtained at slightly different partial pressure conditions with respect to Figure 1f).

4. Discussion

The interactions of free mass-selected gold, silver, and binary silver–gold clusters with CO have been studied in great detail by numerous groups experimentally as well as theoretically (please see references in [9,10,16]). Our results for the trimer cluster carbonyls presented here are in excellent agreement with the concurrent theoretical calculations reported earlier [10]. The tendency of small gold clusters to strongly bind carbon monoxide is also generally recognized. In particular cationic gold clusters with sizes up to seven atoms exhibit CO binding energies clearly larger than 1 eV [12]. The CO bonding strength then quickly decreases and remains approximately constant around 0.7 eV for clusters with 20–65 atoms [12]. Yet, this value is still considerably above the heat of adsorption of CO on an extended gold surface (Au(1 1 0)) which amounts to 0.3 eV [37].

Interestingly, with 0.55 eV the CO adsorption is notably stronger on a silver surface (Ag(1 1 1) [38]) than on the gold surface. However, this relation is reversed for the case of the CO binding to atomic cations (Au$^+$–CO E_b = 2.08 eV [39]; Ag$^+$–CO E_b = 0.93 eV [40]). A similar stronger interaction of CO with gold compared to silver is also observed for the small trimer clusters as can be seen from Figure 2. This trend generally applies to small Ag$_n$Au$_m^+$ in that the CO binding energy to these clusters decreases with increasing silver content [8–10].
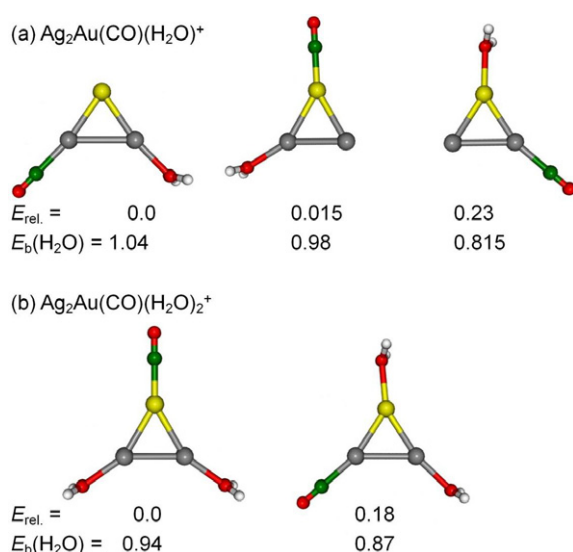
With respect to the structures of the trimer carbonyls theoretical simulations show that each CO molecule binds via the carbon atom in a μ_1-atop position to one metal atom of the small triangular clusters [10,41]. The low temperature CO saturation coverage is three for Ag$_3^+$ and Ag$_2$Au$^+$, but four for Au$_3^+$ [10].

Much less is known about the bonding of water to small gas phase noble metal clusters. Small gold cluster anions were reported to adsorb one water molecule at room temperature and several H_2O molecules at lower temperatures [42]. The complex Au$_3$(H$_2$O)$_3^+$ was detected in our ion trap experiment previously, but no binding energies have been determined so far [36]. Earlier experimental and theoretical studies on the Au(H$_2$O)$^+$ complex revealed binding energies of H_2O to the positively charged gold atom in the range from 1.1 to 1.8 eV [27,39,43,44]. The experimental binding energy of H_2O to Au$_3^+$ determined in this contribution (E_b = 0.98 eV for the 'loose' TS, see Table 2) is slightly below these values.

The theoretical simulations performed in the present study result in a binding energy of 1.20 eV with the water molecule being bound via the more electronegative oxygen atom to a gold atom, in agreement with previous DFT calculations. In the Au$_3^+$–H$_2$O complex, the bound water molecule was found not to change its geometry and the O–H bond length of 0.97 Å is not significantly altered. For larger gold clusters the H_2O bonding strength has been found to further decrease: Theoretical simulations of the neutral cluster Au$_8$ yielded water adsorption energies between 0.3 and 0.6 eV [45]. The calculated Au$_{10}^+$–H$_2$O binding energy is 0.54 eV [46].

No data are available so far concerning the interaction of water with silver clusters or binary silver–gold clusters. Our DFT calculations show that also in these cases the water molecule is bound to
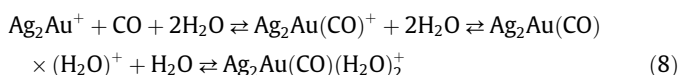
Figure 5. Calculated lowest energy structures of the experimentally detected coadsorption complexes (a) $Ag_2Au(CO)(H_2O)^+$ and (b) $Ag_2Au(CO)(H_2O)_2^+$. Displayed below the structures are also the relative total energies $E_{rel.}$ of the complexes and the binding energies of H_2O $E_b(H_2O)$ (the average binding energies of both H_2O in the case of $Ag_2Au(CO)(H_2O)_2^+$, respectively). All energies are given in units of eV.

the clusters via the oxygen atom and that the H_2O geometry remains nearly unperturbed upon adsorption. Interestingly, the most stable $Ag_2Au(H_2O)^+$ complex has the water molecule bound to a silver atom (as listed in Table 2), while the H_2O interaction is weakened by 0.18 eV, if it is attached to the gold atom of the triangular Ag_2Au^+ cluster.

The composition dependent H_2O binding energy trend observed in the present experiments is similar to that of CO (Figure 2) in that E_b decreases with increasing silver content. However, this trend is much less pronounced for the H_2O binding energies (which are actually quite similar for Ag_3^+ and Ag_2Au^+) and thus, a cross over occurs as apparent from Figure 2. This results in comparable H_2O and CO binding strength to the binary cluster Ag_2Au^+, but a stronger interaction of CO with Au_3^+, in contrast to Ag_3^+, which binds H_2O more strongly. The experimental observations in this respect are well supported by the results of our first principles calculations (Table 2 and Figure 2).

This cross over in E_b with the change in composition is clearly reflected in the results of the coadsorption experiment as shown in Figure 1g-i. The gold trimer reacts to $Au_3(CO)_3^+$, while the silver trimer yields $Ag_3(H_2O)_{1,2}^+$. Apparently, the most strongly bound ligand prevents the coadsorption of the more weakly bound molecule. Similar competitive adsorption effects have been observed also for other ligands on gold clusters previously [47]. In the case of Ag_2Au^+, however, coadsorption of H_2O and CO is indeed detected leading to the complexes $Ag_2Au(H_2O)CO^+$ and $Ag_2Au(H_2O)_2CO^+$ (Figure 1h). The calculated structures of these complexes are depicted in Figure 5. Interestingly, the structures of $Ag_2Au(H_2O)CO^+$ with the water molecule attached to Ag and the CO bound to Au is almost degenerate with the structure, in which both molecules H_2O and CO are attached to silver atoms. In contrast, the binding of H_2O to Au is clearly energetically unfavorable (Figure 5a).

The mechanism of this coadsorption reaction can be deduced from the kinetic measurements shown in Figure 4. The first reaction step is the adsorption of one CO molecule followed by sequential H_2O adsorption:

$$Ag_2Au^+ + CO + 2H_2O \rightleftarrows Ag_2Au(CO)^+ + 2H_2O \rightleftarrows Ag_2Au(CO)$$
$$\times (H_2O)^+ + H_2O \rightleftarrows Ag_2Au(CO)(H_2O)_2^+ \qquad (8)$$

Although the CO binding energy to Ag_2Au^+ is comparable to the H_2O binding energy (cf. Figure 2), the order of magnitude larger CO partial pressure apparently determines the pre-adsorption of CO.

A further interesting aspect is the stoichiometry of the largest observed coadsorption complex $Ag_2Au(CO)(H_2O)_2^+$ (Figure 1h). Because the number of H_2O (CO) molecules corresponds to the number of silver (gold) atoms it might be speculated based on the experiment that these ligands are each attached to one of the respective metal atoms. This structural conjecture is nicely confirmed by the results of our quantum chemical calculations, which are depicted in Figure 5b. The lowest energy structure of $Ag_2Au(CO)(H_2O)_2^+$ is indeed clearly the one with the H_2O molecules adsorbed onto the silver atoms.

Yet, nothing can be deduced from the experimental data about the potential activation and/or reaction of the adsorbed molecules because no fragment loss has been detected in the mass spectra. However, considering the above observation that each molecule is attached to one separate metal atom and that the mechanisms Eqs. (7) and (8) reveal equilibrium reaction kinetics, i.e. the adsorbed CO and H_2O may be lost again, a further interaction of CO with H_2O might be rather unlikely without an additional Langmuir–Hinshelwood type reaction step. In this case the future strategy will be to extend the experiments to larger cluster sizes and in particular to higher temperatures which might help to overcome potential activation barriers involved in the perspective water gas shift chemistry on the binary silver–gold clusters.

5. Conclusion

In this contribution the adsorption and coadsorption behavior of H_2O and CO on pure and binary silver–gold cluster cations $Ag_nAu_m^+(n + m = 3)$ was investigated employing gas phase reaction kinetics measurements in an ion trap and first principles DFT simulations. In particular, for the adsorption of water on the investigated clusters binding energies could be determined for the first time via statistical reaction rate analysis. These results are in favorable agreement with the respective calculated data. The comparison to the CO binding energies revealed a cross over in the binding energy values with H_2O being more strongly bound compared to CO on Ag_3^+, while the reverse was observed for Au_3^+. For Ag_2Au^+ the bonding strength of H_2O and CO are almost identical and only in this case coadsorption is observed resulting in the complexes $Ag_2Au(CO)(H_2O)^+$ and $Ag_2Au(CO)(H_2O)_2^+$.

References

[1] R. Ferrando, J. Jellinek, R.L. Johnston, Chem. Rev. 108 (2008) 845.
[2] J.K. Edwards, E. Ntainjua, A.F. Carley, A.A. Herzing, C.J. Kiely, G.J. Hutchings, Angew. Chem. Int. Ed. 48 (2009) 8512.
[3] D.I. Enache et al., Science 311 (2006) 362.
[4] M. Chen, D. Kumar, C.-W. Yi, D.W. Goodman, Science 310 (2005) 291.
[5] S.M. Lang, T.M. Bernhardt, Phys. Chem. Chem. Phys. 14 (2012) 9255.
[6] K. Koszinowski, D. Schröder, H. Schwarz, Chem. Phys. Chem. 4 (2003) 1233.
[7] M. Neumaier, F. Weigend, O. Hampe, M.M. Kappes, J. Chem. Phys. 125 (2006) 104308.
[8] M. Neumaier, F. Weigend, O. Hampe, M.M. Kappes, Faraday Discuss. 138 (2008) 393.
[9] D.M. Popolan, M. Nößler, R. Mitrić, T.M. Bernhardt, V. Bonačić-Koutecký, Phys. Chem. Chem. Phys. 12 (2010) 7865.
[10] D.M. Popolan, M. Nößler, R. Mitrić, T.M. Bernhardt, V. Bonačić-Koutecký, J. Phys. Chem. A 115 (2011) 951.
[11] M. Okumura, Y. Kitagawa, M. Haruta, K. Yamaguchi, Appl. Catal. A 291 (2005) 37.

[12] M. Neumaier, F. Weigend, O. Hampe, M.M. Kappes, J. Chem. Phys. 122 (2005) 104702.

[13] A. Prestianni, A. Martorana, F. Labat, I. Ciofini, C. Adamo, J. Phys. Chem. B 110 (2006) 12240.

[14] H. Hess, S. Kwiet, L. Socaciu, S. Wolf, T. Leisner, L. Wöste, Appl. Phys. B 71 (2000) 337.

[15] T.M. Bernhardt, Int. J. Mass Spectrom. 243 (2005) 1.

[16] T.M. Bernhardt, J. Hagen, S.M. Lang, D.M. Popolan, L. Socaciu-Siebert, L. Wöste, J. Phys. Chem. A 113 (2009) 2724.

[17] R. Keller, F. Nöhmeier, P. Spädtke, M.H. Schönenberg, Vacuum 34 (1984) 31.

[18] K.A. Holbrook, M.J. Pilling, S.H. Robertson, Unimolecular Reactions, John Wiley & Sons Ltd., Chichester, 1996.

[19] J.I. Steinfeld, J.S. Francisco, W.L. Hase, Chemical Kinetics and Dynamics, Prentice Hall, Upper Saddle River, New Jersey, 1999.

[20] O. Reynolds, Phil. Trans. Roy. Soc. 10 (1879) 727.

[21] J.C. Maxwell, Phil. Trans. Roy. Soc. 170 (1879) 231.

[22] G. Loriot, T. Moran, Rev. Sci. Instrum. 46 (1975) 140.

[23] R.C. Bell, K.A. Zemski, D.R. Justes, A.W. Castleman Jr., J. Chem. Phys. 114 (2001) 798.

[24] P.M. Langevin, Ann. Chem. Phys. 5 (1905) 245.

[25] R. Marcus, J. Chem. Phys. 43 (1965) 2658.

[26] L. Drahos, K. Vekey, J. Mass Spectrom. 36 (2001) 237.

[27] D. Feller, E.D. Glendening, W.A. de Jong, J. Chem. Phys. 110 (1999) 1475.

[28] Y. Shi, V.A. Spasov, K.M. Ervin, J. Chem. Phys. 111 (1999) 938.

[29] A.D. Becke, J. Chem. Phys. 38 (1988) 3098.

[30] A.D. Becke, J. Chem. Phys. 98 (1993) 5648.

[31] C. Lee, W. Yang, R.G. Parr, Phys. Rev. B 37 (1988) 785.

[32] B. Miehlich, A. Savin, H. Stoll, H. Preuss, Chem. Phys. Lett. 157 (1989) 200.

[33] K. Eichkorn, F. Weigend, O. Treutler, R. Aldrichs, Theor. Chim. Acta 97 (1997) 119.

[34] D. Andrea, U. Haeussermann, M. Dolg, H. Stoll, H. Preuss, Theor. Chim. Acta 77 (1990) 123.

[35] A. Schäfer, H. Huber, R. Ahlrichs, J. Chem. Phys. 100 (1994) 5829.

[36] S.M. Lang, T.M. Bernhardt, Int. J. Mass Spectrom. 286 (2009) 39.

[37] J.M. Gottfried, K.J. Schmidt, S.L.M. Schroeder, K. Christmann, Surf. Sci. 536 (2003) 206.

[38] G. McElhiney, H. Papp, J. Pritchard, Surf. Sci. 54 (1976) 617.

[39] D. Schröder, H. Schwarz, J. Hrusak, P. Pyykkö, Inorg. Chem. 37 (1998) 624.

[40] F. Meyer, Y.-M. Chen, P.B. Armentrout, J. Am. Chem. Soc. 117 (1995) 4071.

[41] A. Fielicke, G. von Helden, G. Meijer, D.B. Pedersen, B. Simard, D.M. Rayner, J. Am. Chem. Soc. 127 (2005) 8416.

[42] W.T. Wallace, R.B. Wyrwas, A.J. Leavitt, R.L. Whetten, Phys. Chem. Chem. Phys. 7 (2005) 930.

[43] L. Poisson, P. Pradel, F. Lepetit, F. Réau, J.-M. Mestdagh, J.-P. Visticot, Eur. J. Phys. D 14 (2001) 89.

[44] L. Poisson, F. Lepetit, J.-M. Mestdagh, J.-P. Visticot, J. Phys. Chem. A 106 (2002) 5455.

[45] A. Bongiorno, U. Landman, Phys. Rev. Lett. 95 (2005) 106102.

[46] M. Okumura, M. Haruta, Y. Kitagawa, K. Yamaguchi, Gold Bull. 40 (2007) 40.

[47] S.M. Lang, T.M. Bernhardt, Eur. J. Phys. D 52 (2009) 139.